JMEPEG (2018) 27:2741–2746
https://doi.org/10.1007/s11665-018-3361-3

1059-9495/$19.00

Synthesis of Self-Assembled rGO-Co_3O_4 Nanoparticles in Nanorods Structure for Supercapacitor Application

Soumita Jana, Neha Singh, Arnab Sankar Bhattacharyya, and Gajendra Prasad Singh

(Submitted April 20, 2017; in revised form March 12, 2018; published online April 19, 2018)

A simple hydrothermal process was used to design self-assembled Co_3O_4 nanoparticles in nanorod structure in the presence of graphene oxide as a template. The as-prepared Co_3O_4 sample in a loose powder form was calcined at 450 °C to get the well-crystalline phase of the same compound. The obtained Co_3O_4 powder sample was characterized by using the powder XRD and SEM. The XRD pattern shows totally nine distinct reflection peaks of (111), (220), (311), (222), (400), (422), (511), (440), and (533) planes. The most intense peaks were chosen to evaluate the structural parameters. The lattice parameters (*a*), volume (V), and density (ρ) of the samples are 8.09 Å, 529.47 Å^3, 6.06 g/cc, which are comparable to the value of lattice parameter (a = 8.056 Å), volume (V = 528.30 Å^3), and density (ρ = 6.055 gm/cc) for bulk Co_3O_4. The average size of the Co_3O_4 nanoparticles is 14 nm which is smaller than the SEM size of 50 nm corresponding to the agglomeration of tiny particles. Further, the formation of Co_3O_4 nanoparticles were also confirmed by obtaining the band at 569, 1334,1337, 1566, and 3397 cm^{-1} in FTIR spectrum. Totally five characteristics peaks from Co_3O_4 at 182.57, 456.49, 505.84, 605.80, and 618.02 cm^{-1} and peaks from GO-Co_3O_4 at 182.57, 483.44, 505.84, 605.80, and 618.02 cm^{-1} corresponding to F_{2g}, E_g, F_{2g}, F_{2g}, and A_g modes of the crystalline Co_3O_4, respectively, in the Raman spectra. In the case of GO-Co_3O_4 composite, low-intensity peaks of D and G bands are observed. The specific capacitance in rGO-Co_3O_4 nanocomposite is about 65.15 Fg^{-1}.

Keywords cobalt oxide, graphene, hydrothermal, supercapacitors

1. Introduction

Energy is one of the most important problems that the human race may face in near future (Ref 1). This energy crisis has led to renewable energy conversion and storage systems. Due to the outburst of electronic gadgets like tablets, smartphones, and e-readers, the demand of power sources of portable electronic devices has increased in recent years. However, it is hard to create a miniature energy device without limiting its power capacity (Ref 2, 3). Electrochemical energy storage technologies include batteries, fuel cells, and electrochemical capacitors (ECs). ECs can deliver higher energy density than batteries. ECs can be characterized from batteries based on their operational characteristics, i.e., (1) symmetrical (high reversibility) and sloping charge-discharge profiles, (2) very short charge-discharge time (a few seconds), (3) exceptional cycle life, and (4) continuous variation of free energy with the degree of conservation. ECs are also known as supercapacitors. Based on the energy storage mechanism, supercapacitors are classified in to two types: electric double-layer capacitors (EDLCs) and pseudocapacitors (Ref 1-8).

EDLCs are made of carbon-based materials such as carbon nanotubes and reduced graphene oxide (Ref 9-11). This type of supercapacitor stores more electrical energy by electrostatic accumulation of charges in the electric double layer and releases energy by charge separation at the interface between electrode and electrolyte (Ref 12-15). However, metal oxides like MnO_2, RuO, and NiO and conducting polymers have been used to build pseudocapacitors with high specific capacitance, and these pseudocapacitors, taking advantages of the reversible Faradaic reactions occurring at the electrode surface, offer better electrochemical performances than the EDLCs (Ref 2, 10, 19).

Nowadays, transition metal cobalt and cobalt oxide (Co_3O_4) are known as promising materials due to their huge applications in gas sensing, lithium-ion batteries, data storage, catalyst, and electrochromic devices (Ref 2-7, 20). Among all the transition metal oxide candidates, Co_3O_4 is recognized to be ideal due to its high theoretical capacitance (3560 F/g), environmental friendliness, and electrochemical performance. Co_3O_4 is an important magnetic p-type semiconductor, which belongs to the normal spinel crystal structure based on a cubic close-packing array of oxide ions, in which Co (II) ions occupy the tetrahedral 8a sites and Co (III) ions occupy the octahedral 16d sites. Co also has comprehensive studies due to its different crystal structures and its structure-dependent electronic and magnetic properties (Ref 4, 6). Various methods like sol-gel method, thermal decomposition of solid phase, hydrothermal method, solvothermal decomposition, liquid control precipitation method, chemical vapor deposition, and spray pyrolysis were experimented to synthesized nanosized spinel Co_3O_4 (Ref 6). Among all the kinds of synthesis techniques, hydrothermal/solvothermal method has achieved great success. Co_3O_4

Soumita Jana and **Gajendra Prasad Singh,** Centre for Nanotechnology, Central University of Jharkhand, Brambe, Ranchi, Jharkhand 835205, India; **Neha Singh,** Centre for Applied Chemistry, Central University of Jharkhand, Brambe, Ranchi, Jharkhand 835205, India; and **Arnab Sankar Bhattacharyya,** Centre for Nanotechnology, Central University of Jharkhand, Brambe, Ranchi, Jharkhand 835205, India and Centre of Excellence in Green and Efficient Energy Technology (CoE-GEET), Central University of Jharkhand, Brambe, Ranchi, Jharkhand 835205, India. Contact e-mail: gpsinghcuj@gmail.com.

nanomaterials have various morphologies, such as nanoparticles, nanospheres, nanorods, nanowires, nanosheets, nanocubes, nanocrystalline, nanorod bunches, and all have been studied for supercapacitor materials (Ref 6, 8, 25, 26).

Several methods have been proposed to improve the electrical conductivity of Co_3O_4-based materials (Ref 25, 26). One of them is to hook Co_3O_4 onto graphene sheets to create hybrid nanostructures (Ref 9). Graphene has been studied largely as an ideal matrix for the growth of metal nanoparticles owing to its high conductivity, electrochemical stability, high surface area (a theoretical value of 2630 m^2g^{-1}) (Ref 9, 11), great flexibility, excellent mechanical properties, and rich chemistry (Ref 5, 9). Co_3O_4/graphene nanocomposites efficiently enhance the conductivity by a synergetic effect which leads to high electrocatalytic performance (Ref 2-6). Graphene as a new carbon material has attracted much attention since it was isolated from graphite in layer-by-layer manner (Ref 12, 16-18). It is a promising electrode candidate for EDLCs due to its superb characteristics including the excellent mechanical strength (Ref 16). Recently, many researchers have constructed a graphene-based metal oxide structure. It was found that the composites showed improved performance with higher electron transport rate, electrolyte contact area, and structural stability (Ref 16-18). It can be attributed to the special composite structure in which metal oxides are attached on the surface or intercalated into the interlayer of large patches of graphene (Ref 16-19). In this paper, we proposed the synthesis of self-assembled GO-Co_3O_4 nanoparticles in nanorods structure.

2. Experimental Process

2.1 Materials

Analytical-grade graphite flake was procured from Alfa Aeser, and cobalt chloride hexahydrate ($CoCl_2.6H_2O$) and urea (NH_2CONH_2) were purchased from Sigma-Aldrich. Other chemicals such as sodium nitrate ($NaNO_3$), sulphuric acid (95-97%), $KMnO_4$, HCl, and hydrogen peroxide (30%, H_2O_2) were procured from Fisher Scientific. All chemicals were used without further purification.

2.2 Synthesis of Graphene Oxide Sheets

Graphene oxide was synthesized from commercial graphite flakes by using the well-known modified Hummer's method. In a typical process, graphite flakes (2 g) and $NaNO_3$ (1 g) were mechanically mixed. The mixture was poured into concentrated H_2SO_4 (46 ml, 18 M), and temperature was maintained at 0 °C using ice bath. $KMnO_4$ (6 g) was slowly added to the resultant solution under vigorous stirring. Addition of $KMnO_4$ gradually increased the temperature and was maintained below 20 °C in the ice bath so as to produce the graphite oxide. After complete addition of $KMnO_4$, the reaction mixture was warmed to 35 °C in an oil bath and maintained at this temperature with stirring until brown color paste is formed. Thereafter, the reaction was terminated slowly by adding water (92 ml), which increased the temperature to between 95 and 98 °C, and resulting suspension was maintained at this temperature for 20 min. The suspension was then diluted to approximately 280 ml by the addition of water followed by treatment with H_2O_2 (9 ml, 33%). Upon treatment with peroxide, the suspension turned bright yellow. After cooling in air, the suspension was filtered and washed with aqueous HCL (1:10, 37%) and water. The obtained solid was graphite oxide. The graphite oxide was further exfoliated by sonicating in water for 2 h and then it was centrifuged at 4500 rpm for 20 min. The supernatant was decanted and oven-dried at 50 °C temperature for 12 h, and the obtained black powder was named as GO.

2.3 Synthesis of Reduced Graphene Oxide (rGO)-Co_3O_4 Nanocomposites

In this process, firstly an aqueous solution of $CoCl_2.6H_2O$ (1 mmol) and urea (1 mmol) were prepared separately of total 80 ml by volume in water and stirred for 10 min. Both solutions were mixed homogeneously under vigorous stirring for 30 min. Then the mixed solution was added into the aqueous GO solution. The whole mixture was transferred in to a Teflon-lined stainless steel autoclave of 100-ml capacity. The Teflon-lined autoclave was kept in muffle furnace at 120 °C for 16 h. After cooling to room temperature, the light pink precipitate was obtained after filtration. The resultant powder was washed several times with deionized water and dried at 50 °C. Finally, the powder was heated at 450 °C for 2 h to get the rGO-Co_3O_4 nanoparticles assembled in a specific nanorod structure.

2.4 Material Characterization

The structural analysis of the derived composites was carried out by x-ray diffraction system (Rigaku SmartLab) equipped with Cu Kα (λ = 1.5406 Å). The morphological analysis was conducted using Carl Zesis ULTRA55 FESEM

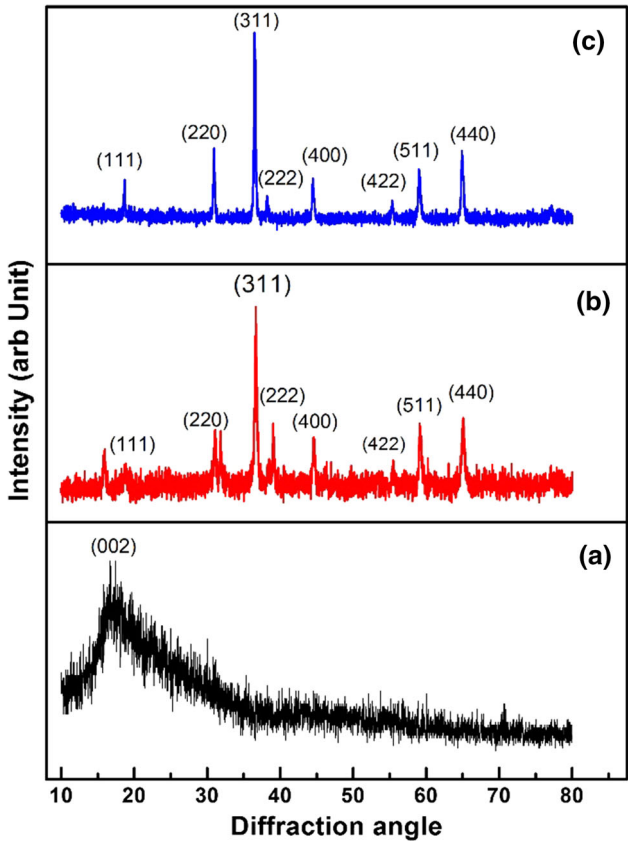

Fig. 1 X-ray diffraction patterns of the (a) GO (b) Co_3O_4 and (c) rGO-Co_3O_4 nanocomposites

Table 1 Interplaner spacing (*d*) and intensity distribution of Co_3O_4 and GO-Co_3O_4

Interplaner spacing, d_{hkl}, nm			Intensity (Ip)	
Co_3O_4	rGO-Co_3O_4	*(h k l)*	Co_3O_4	rGO-Co_3O_4
0.469	0.471	*(1 1 1)*	26	29
0.282	0.289	*(2 2 0)*	42	43
0.247	0.246	*(3 1 1)*	100	100
0.230	0.234	*(2 2 2)*	45	20
0.203	0.203	*(4 0 0)*	40	26
0.166	0.166	*(4 2 2)*	27	17
0.156	0.156	*(5 1 1)*	45	32
0.144	0.144	*(4 4 0)*	47	38

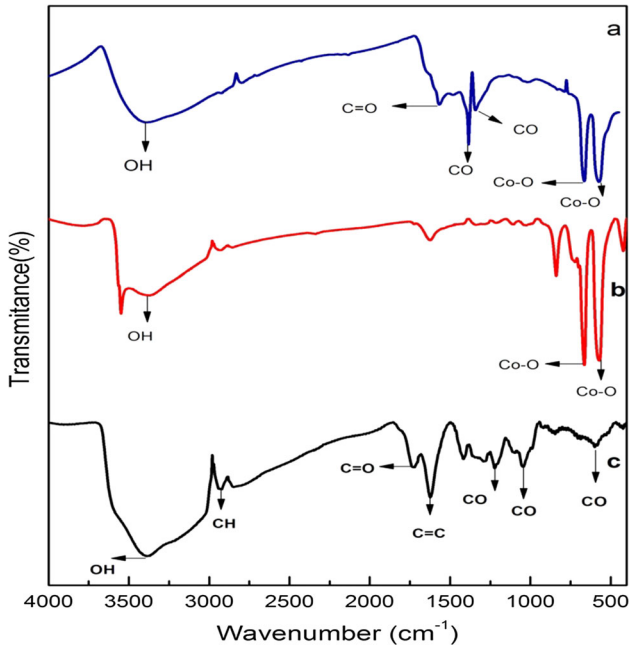

Fig. 2 FTIR spectra of (a) rGO-Co_3O_4 (b) Co_3O_4 (c) GO

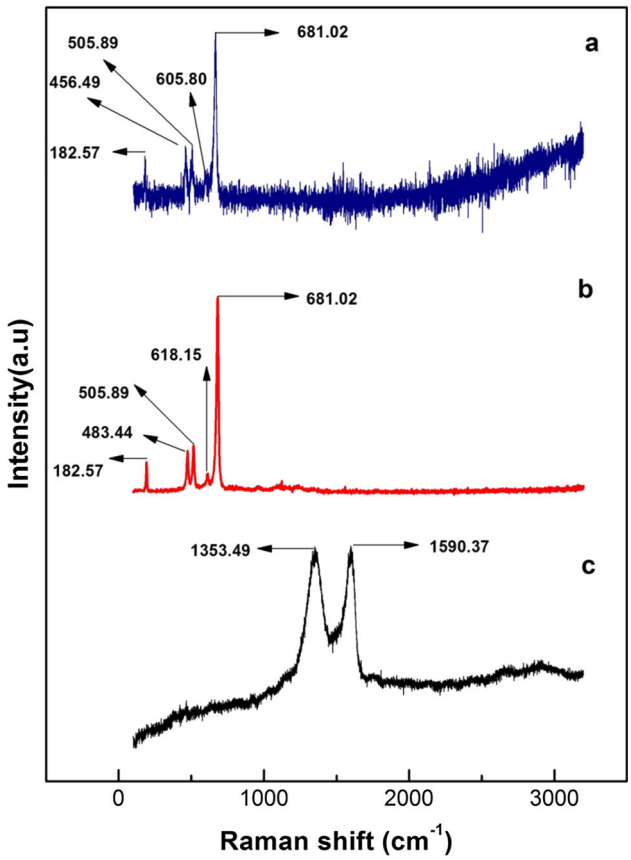

Fig. 3 Raman spectra of (a) rGO-Co_3O_4 (b) Co_3O_4 and (c) GO

scanning electron microscope (SEM). A Fourier transform infrared (FTIR) study was also carried out using Perkin Elmer FTIR spectroscopy to examine the vibrational characteristics of graphene oxide, cobalt oxide nanoparticles, and composite materials. UV-Vis spectroscopy study was carried out using PerkinElmer UV/VIS Spectrometer Lambda 35. The room-temperature Raman spectra were obtained on loose powder with an iHR550 Raman spectrophotometer, Horiba Jobin Yvon, with a He-Ne laser (632.8 nm) as the excitation source. The cyclic voltammetry (CV) tests were carried out with a CHI660E electrochemical workstation (CH Instruments Inc., China) in a conventional three-electrode cell which contains the working electrode, counterelectrode (Pt), and reference electrode (Ag/AgCl electrode) in 2 M KOH electrolyte solution with in the potential window of − 1.5 to 1.5 V

3. Result and Discussion

Figure 1 shows the x-ray diffraction patterns of GO, Co_3O_4 nanoparticles and rGO-Co_3O_4 nanocomposite samples. The characteristic diffraction pattern of (002) reflection plane of GO is observed at 16.65° (Ref 23, 24). The diffraction peaks of Co_3O_4 nanoparticles observed at 18.88°, 30.98°, 36.64°, 39.00°, 45.45°, 59.21°, 64.77°, and 77.06° were assigned to the reflection from the crystal planes of (111), (220), (311), (400), (422), (511), (440), and (533) which are in good agreement with the typical *fcc* spinel Co_3O_4 (JCPDS card No. 43-1003) (Ref 2, 3, 5, 25, 26). The lattice parameters (*a*), volume (V), and density(ρ) of Co_3O_4 are 8.09 Å, 529.47 Å^3, 6.06 g/cc are comparable to the value of $a = 8.056$ Å, $V = 528.30$ Å^3 and $\rho = 6.055$ gm/cc for bulk Co_3O_4 (as given in Table 1).

In rGO-Co_3O_4 nanocomposites, the marginal shifts toward lower diffraction angle were noticed in the diffraction peaks of

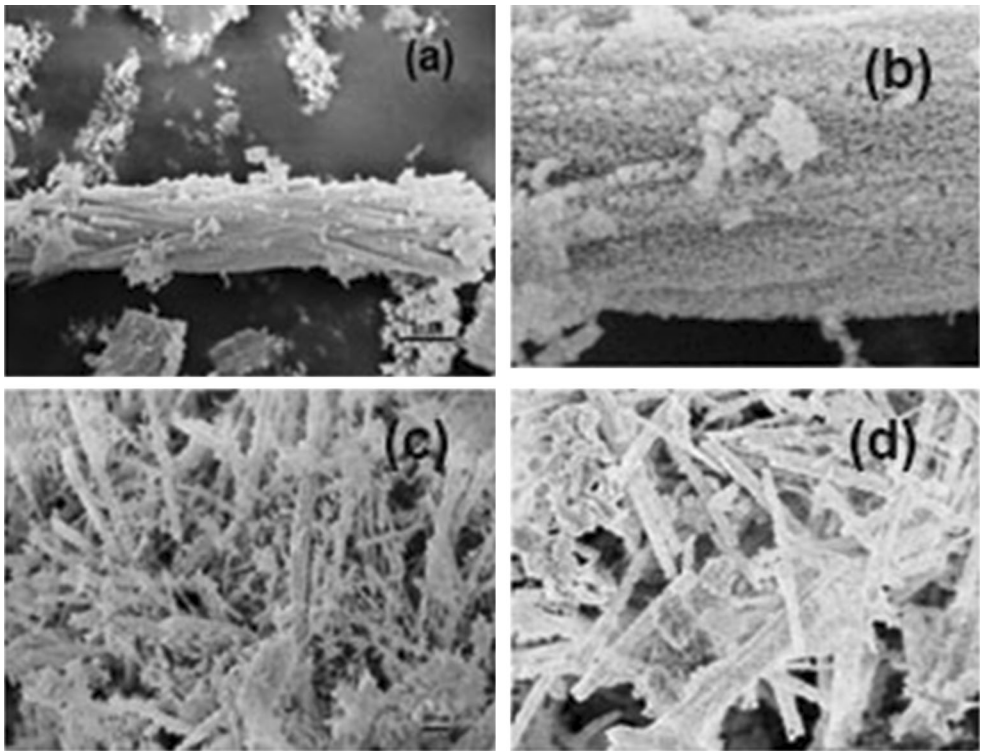

Fig. 4 SEM micrographs of (a) Co_3O_4 (b) Enlarge view of (a), (c) rGO-Co_3O_4 nanocomposites, and (d) enlarge view of (c)

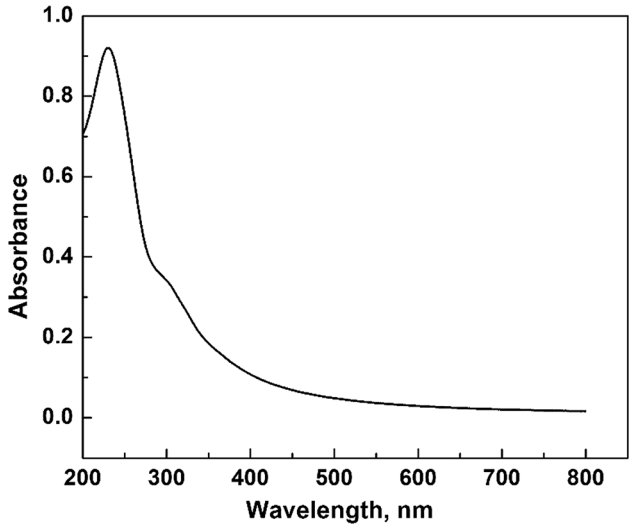

Fig. 5 UV-Vis absorption spectra of GO

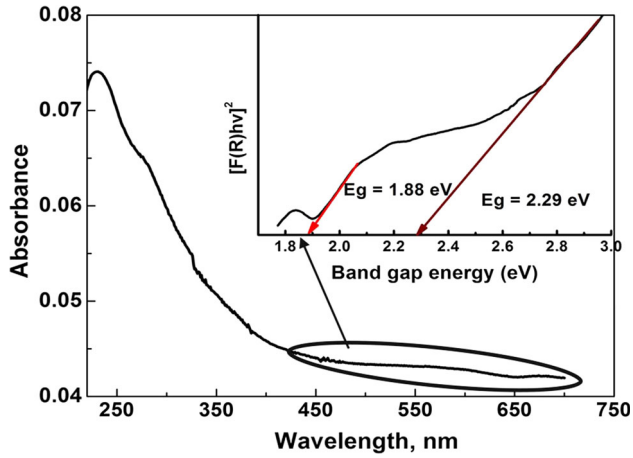

Fig. 6 UV-Vis absorption spectra of rGO-Co_3O_4

Co_3O_4. No peak of graphene is observed in the rGO-Co_3O_4 nanocomposite. It could be due to either the amount of GO is less than the critical limit or very low intensity in comparison with the diffraction intensity of Co_3O_4 nanoparticles. An average size of about 14 nm of the Co_3O_4 nanoparticles is calculated using Scherer's formula $D = \frac{0.9\lambda}{\beta.Cos\theta}$.

FTIR spectra of GO and rGO-Co_3O_4 nanocomposites in the range of 400-4000 cm^{-1} are shown in Fig. 2. The characteristic peaks of GO are observed at 3385, 2925, 1735, 1625, 1212, 1042, and 584 cm^{-1}, which were assigned to O-H, CH, C = O, C = C, C-O, C-O, and C-O groups available in oxidized samples. In case of Co_3O_4 nanoparticles (Fig. 2b), the peaks due to O-H, Co-O, and Co-O appeared at 3398, 660, and 548 cm^{-1}, whereas for rGO-Co_3O_4, the peaks of Co-O and Co-O appeared at 668 and 578 cm^{-1} along with the peaks of O-H, asymmetric C-O, symmetric C-O at 3397, 1566, 1337, 1334 cm^{-1} which confirmed the formation of the rGO-Co_3O_4 nanocomposites (Ref 9, 21).

Raman spectroscopy is a powerful nondestructive tool to characterize the complex materials. The Raman spectra of the GO, Co_3O_4, and GO-Co_3O_4 nanocomposites are portrayed in Fig. 3 in the range of 0-3000 cm^{-1}. In GO sample (Fig. 3c), the D and G peaks are observed at 1353.49 and 1590.37 cm^{-1} (Ref 22), respectively. All signals in pure Co_3O_4 and rGO-Co_3O_4 nanocomposites correspond to the vibrational modes in spinal Co_3O_4. Totally five Raman signals in Co_3O_4 were observed at 182.57, 456.49, 505.84, 605.80, and 618.02 cm^{-1},

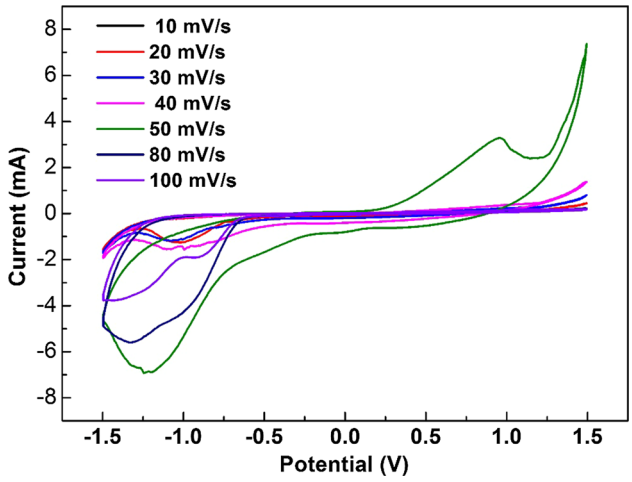

Fig. 7 CV curves of GO at different scan rate

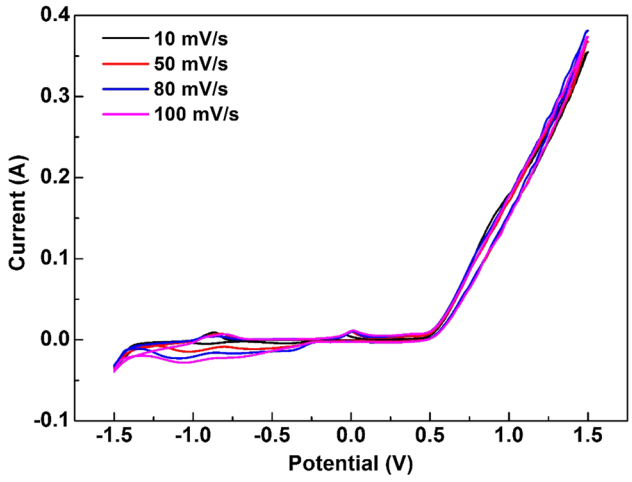

Fig. 8 CV curves of rGO-Co_3O_4 at different scan rate

whereas in GO-Co_3O_4 the signals were observed at 182.57, 483.44, 505.84, 605.80, and 618.02 cm^{-1} that correspond to F_{2g}, E_g, F_{2g}, F_{2g}, and A_g modes of the crystalline Co_3O_4, respectively, (Ref 3, 21).

The morphology of GO and rGO-Co_3O_4 nanocomposites was investigated by SEM and is shown in Fig. 4. It is observed that the particles are about 50 nm size (Fig. 4a). Each particle is self-assembled in a specific nanorod structure of about 300 µm length. The enlarged view of Fig. 4(a) is shown in Fig. 4(b). Figure 4(c), (d) shows the normal and enlarged view of the SEM micrograph of rGO-Co_3O_4 nanocomposites. The micrographs reveal that the GO helps to break the agglomeration or bunch of Co_3O_4 nanoparticles without disturbing the particles assembly of nanorods (Ref 3).

Figure 5 shows the UV absorption spectra of graphene oxide (GO). The two bands in GO sample are observed at 232 nm and about 300 nm. The peak at 232 nm is attributed to π-π^* transitions of C = C in carbon system, and the additional broad shoulder peak at 300 nm is due to n-π^* transition of C = O (Ref 21). Moreover, the rGO-Co_3O_4 nanocomposites absorption spectrum is shown in Fig. 6. The absorption bands were observed at 232, 300, 550, and 670 nm. The first two bands arose due to the presence of GO in the composite. The bands at 550 nm, on the other hand, arose due to intervalence charge transfer in Co_3O_4 (Co^{2+} to Co^{3+} or vice versa). The absorption peaks observed at 670 nm indicate the ligand-metal charge transfer process O^{2-}/Co^{3+} and O^{2-}/Co^{2+}, respectively. The bang gap energy plot of the marked region contributed by Co_3O_4 nanoparticles is shown in the inset of Fig. 6. It is observed that the Co_3O_4 nanoparticles have two optical band gaps (Eg). One is at 1.88 eV associated with the O^{2-}/Co^{2+} charge transfer, whereas the other band gap energy at 2.29 eV relates to the O^{2-}/Co^{3+} charge transfer.

Figures 7 and 8 display the CV curves of GO and rGO-Co_3O_4 at different scan rate in 2 M KOH electrolyte solution with in the potential window of − 1.5 to 1.5 V. The result indicates a specific capacitance with the GO electrode. Now the specific capacitance of the electrode can be calculated as, $C = \frac{(\int I.dV)}{v.m.V}$ (Ref 22), where C is specific capacitance of the electrode material, I is response current (A), V is potential (V), v is scan rate (mV/Sec), and m is mass of the electrode material (gm). The specific capacitances of GO are 6.54, 1.11, 0.715, 0.854, 1.27, 2.15, 0.674, and 0.320 Fg^{-1} at different scant rates 5, 10, 20, 30, 40, 50, 80, and 100 mV/s, respectively. Evidently, the area surrounded by the CV curve is dramatically enhanced by the introduction of GO in Co_3O_4. The maximum specific capacitance obtained is about 65.15 Fg^{-1} at a scan rate of 50 mV/s.

4. Conclusions

The GO films were successfully synthesized by Hummer's method which was used in electrode material of supercapacitor application and also used to produce composite materials to enhance the specific capacitance of supercapacitors. Self-assembled Co_3O_4 and GO-Co_3O_4 composites were synthesized by the hydrothermal process. Formation of Co_3O_4 was confirmed by FTIR, Raman spectra, and XRD. SEM image showed the porous structure of Co_3O_4 particles and nanorod-like structure of Co3O4 particles in the presence of GO which is beneficial for efficient electrochemical activity useful for supercapacitors. The specific capacitance in rGO-Co_3O_4 nanocomposite is obtained about 65.15 Fg^{-1}.

Acknowledgments

Authors express sincere thanks to Centre of Excellence in Green and Efficient Energy Technology, Central University of Jharkhand, INUP Program (IISc Bangalore), for providing the measurement facilities. This work was fully supported by the SERB, Department of Science and Technology, New Delhi, India, under Fast Track Project (SR/FTP/ETA-0028/2011).

References

1. A.K. Mishra and S. Ramaprabhu, Functionalized Graphene-Based Nanocomposites for Supercapacitor Application, *J. Phys. Chem.*, 2011, **115**, p 14006–14013
2. Q. Liao, N. Li, S. Jin, G. Yang, and C. Wang, All-Solid-State Symmetric Supercapacitor Based on Co_3O_4 Nanoparticles on Vertically Aligned Graphene, *ACS Nano*, 2015, **9**(5), p 5310–5317
3. X. Dong, H. Xu, X.W. Wang, Y. Huang, M. Chan-Park, H. Zhang, L. Wang, W. Huang, and P. Chen, 3D Graphene-Cobalt Oxide Electrode

for High-Performance Supercapacitor and Enzyme Less Glucose Detection, *ACS Nano*, 2012, **6**(4), p 3206–3213
4. H. Gao, F. Xiao, C.B. Ching, and H. Daun, High-performance Asymmetric Supercacitor Based on Graphene Hydrogel and Nanostructured MnO_2, *ACS Appl Mater Interfaces*, 2012, **4**, p 2801–2810
5. Y. Kuibo, S. Litao, and C. Liang, Facile Low-Temperature Synthesis of Graphene-Co_3O_4 Nanocomposite and Its Electrochemical Properties, 2014, **20**, p 1–12
6. Y.P. Yang, K.L. Huang, R.S. Liu, L.P. Wang, W.W. Zeng, and P.M. Zhang, Shape-Controlled Synthesis of Nanocubic Co_3O_4 by Hydrothermal Oxidation Method, *Trans. Nonferrous Met. Soc. China*, 2007, **17**, p 1082–1086
7. H. Liu, X. Gou, Y. Wang, X. Du, C. Quan, and T. Qi, Cauliflower-Like Co_3O_4/Three-Dimensional Graphene Composite for High Performance Supercapacitor Applications, *J. Nanomater.*, 2015, **2015**, p 1–9
8. K. Deori, S.K. Ujjain, R.K. Sharma, and S. Deka, Morphology Controlled Synthesis of Nanoporous Co_3O_4 Nanostructures and Their Charge Storage Characteristics in Supercapacitor, *ACS Appl. Mater. Interfaces*, 2013, **5**, p 10665–10672
9. Y. Yao, Z. Yang, H. Sun, and S. Wang, Hydrothermal Synthesis of Co_3O_4-Graphene for Heterogeneous Activation of Peroxymonosulfate for Decomposition of Phenol, *Ind. Eng. Chem. Res.*, 2012, **51**, p 14958–14965
10. M. Khan, M.N. Tahir, S.F. Adil, H.U. Khan, M.R.H. Siddiqui, A.A. Al-warthan, and W. Tremel, Graphene Based Metal and Oxide Nanocomposites: Synthesis, Properties and Their Applications, *J. Mater. Chem. A*, 2015, **3**, p 18753–18808
11. S. Chen, R. Ramachandran, V. Mani, and R. Saraswathi, Recent Advancements in Electrode Materials for the High Performance Electrochemical Super Capacitors, *Int. J. Electrochem. Sci.*, 2014, **9**, p 4072–4085
12. V.V.N. Obreja, *Super Capacitor Specialties-Material Review*, AIP Publishing, Melville, 2014, p 98–120
13. W. Munchgesang, P. Meisner, and G. Yushin, *Super Capacitors Specialties- Technology Review*, AIP Publishing, Melville, 2014, p 196–203
14. M.S. Halper and J.C. Ellenbogen, *Super Capacitors- A Brief Overview, MITRE Nano System Group*, McLean, VA, 2006, p 1–29
15. P. Russo, A. Hu, and G. Compagnini, Synthesis Properties and Potential Applications of Porous Graphene. A Review, *Nano-Micro Lett.*, 2013, **5**(4), p 260–273
16. Y.B. Tan and J. Lee, Graphene for Super Capacitor Applications, *J. Mater. Chem.*, 2013, **1**, p 14814–14843
17. G. Pandolfo and A.F.H. Kamp, Carbon Properties and Their Role in Super Capacitors, *J. Power Source*, 2006, **157**, p 11–27
18. A. Janes, H. Kurig, and E. Lust, Characterization of Activated Nanoporous Carbon for Super Capacitor Electrode Materials, *Carbon*, 2007, **45**, p 1226–1233
19. T. Hsien, C. Chuang, W. Chen, J. Huong, W. Chen, and C. Shu, Hydrous Ruthenium Dioxide/Multi-Walled Carbon Nanotube/ Titanium Electrodes for Super Capacitors, *Carbon*, 2012, **50**, p 1740–1747
20. M. Zhi, C.C. Xiang, J. Han Li, and N. Wu, Nano Structured Carbon-Metal Oxide Composite Electrode for Super Capacitors Review, *R. Soc. Chem.*, 2013, **5**, p 72–88
21. L.H. Ai and J. Jiang, Rapid Synthesis of Nanocrystalline Co_3O_4 by a Microwave-Assisted Combustion Method, *Powder Technol.*, 2009, **195**, p 11–14
22. W. Liu, X. Yan, J. Lang, C. Peng, and Q. Xue, Flexible and Conductive Nanocomposite Electrode Based on Graphene Sheets and Cotton Cloth for Supercapacitor, *J. Mater. Chem.*, 2012, **22**, p 17245–17253
23. Y. Zhu, S. Murali, W. Cai, X. Li, J. Won Suk, J.R. Potto, and R.S. Ruoff, Graphene and Graphene Oxide: Synthesis Properties and Applications, *Adv. Mater.*, 2010, **22**, p 1–99
24. J. Song, X. Wang, and C. Chang, Preparation and Characterization of Graphone Oxide, Hindanli. J. Nanomater., 2014, p 1–6
25. Y.P. Yang, K.L. Huang, R.S. Liu, L.P. Wang, W.W. Zeng, and P.M. Zhang, Shape-Controlled Synthesis of Nanocubic Co_3O_4 by Hydrothermal Oxidation Method, *Trans. Nonferrous Met. Soc. China*, 2007, **17**, p 1082–1086
26. I. Luisetto, F. Pepe, and E. Bemporad, Preparation and Characterization of Nano Cobalt Oxide, *J. Nanoparticle Res.*, 2008, **10**, p 59–67